

## VACUUM SYSTEM FOR THE 8 GeV STORAGE RING

S.H.Be, S.Yokouchi, Y.Morimoto, H.Sakamoto, Y.P.Lee\*, and Y.Oikawa

RIKEN-JAERI Synchrotron Radiation Facility Design Team  
2-28-8, Honkomagome, Bunkyo-ku, Tokyo, 113 Japan

### ABSTRACT

A vacuum system of the 8 GeV storage ring, which is planned by RIKEN-JAERI SRF design team, is presented. The vacuum system is designed so as to maintain the beam-on operating pressure of 1 nTorr or less to achieve an electron (or positron) beam life of approximately 24 hours. We put special emphasis, in this report, on the various vacuum chamber components, flexible vacuum chamber for an insertion device with a RF contact. A stress analysis of the chamber, and crotch together with thermal analysis are discussed.

### 1. INTRODUCTION

The 8 GeV storage ring is a highly brilliant synchrotron radiation source which is presently under conceptual design, and scheduled for initial operation in 1995. The vacuum system forms approximately a 455 m-diameter ring, and consists of two different shaped aluminum alloy chamber extrusions, two types of absorbers, and the various chamber components.

To achieve the beam lifetime of approximately 24 hours, the vacuum chamber with its pumping system is designed so as to maintain the beam-on pressure of 1 nTorr or less.

The main pumping system is based on the non evaporable getter (NEG) strips, installed in the antechamber which runs along almost of the straight section chamber, and a distributed ion pump (DIP) in the bending magnet chamber. Lumped NEG pump, sputter ion pump (SIP) and titanium sublimation pump (TSP) are used at the crotch and absorber locations.

In the storage ring, the maximum achievable beam current depends greatly on the impedance of the vacuum chamber and its components, and RF cavities. A special effort must be given to minimize their impedance characteristics. Therefore, we designed so as to avoid as much as possibly any change in the cross section of the chamber, including its vacuum chamber components.

We report the vacuum system and its current status of development, including vacuum chamber components.

### 2. VACUUM CHAMBER

A cross-sectional view of the vacuum chamber for the straight sections is shown in Fig. 1. The aluminum alloy (A6063-T6) chamber extrusion consists of an electron beam chamber and a slot-isolated antechamber in which NEG strips are installed. SR is almost intercepted by crotches and absorbers placed just downstream and upstream of a bending magnet, and is designed so as not to intercept with the vacuum chamber all around the storage ring.

#### 2.1 Bakeout and Cooling

To achieve the temperature for the NEG activation, a heating current of 60 A is required

\* On leave from Research Institute of Industrial Science and Technology, Korea

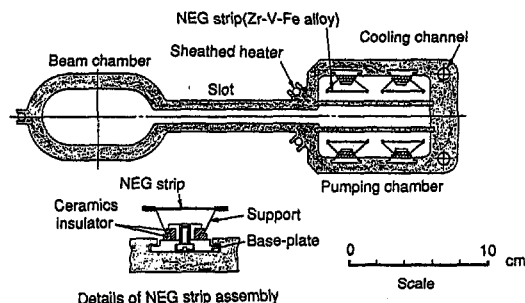


Figure 1. Cross-sectional view of the vacuum chamber for the straight section.

and the corresponding power dissipation is  $4 \text{ m} \times 345 \text{ W/m} (=1380 \text{ W})$ . This thermal load can be easily removed by the water cooling system, which is designed for load up to 5 kW/m. This can be achieved by flowing water at about 2 m/s in two channels of 10mm-diameter.

Bakeout of the chamber is achieved by inserting flexible sheathed heaters in three channels, which can bring the chamber temperature up to 150 °C. The chamber is thermally insulated with kapton films to reduce heat losses. The chamber components such as gauge, valve, bellows and RF cavity are baked using electrical heating tapes.

#### 2.2 Stress Analysis of the Vacuum Chamber

The vacuum chamber must be designed so as to stand the pressure difference between on one side the atmospheric pressure and on the other vacuum. To check this, we analyzed a stress of the vacuum chamber, and its calculation result is shown in Fig. 2. From this figure, it can be seen that the maximum displacement is 0.45 mm at the slot, and the maximum stress is 2.6 kg/mm<sup>2</sup>. The value of stress is less than an allowable stress of 6.8 kg/mm<sup>2</sup> for the aluminum alloy to be used as chamber material. Thus, the vacuum chamber will be

withstand the pressure difference between the atmospheric pressure and the vacuum. However, the displacement is larger than the mounting

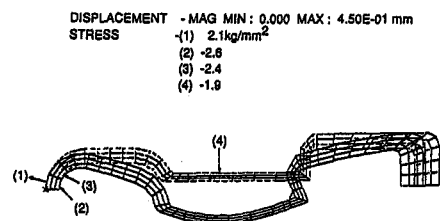


Figure 2. Calculation results of stress analysis

accuracy of

0.1 mm required for beam position monitors (BPM). To reduce the displacement, we are considering a special BPM chamber of a larger wall thickness than that of a present chamber

### 3. CROTCH AND THERMAL ANALYSIS

The SR-induced gas load distribution is mainly based on the percentage of the SR intercepted by the crotch (Cr) and absorber (Ab) placed just downstream and upstream of the bending magnet from where photons are produced. A schematic diagram of one cell including Cr, Ab and the chamber components is shown in Fig.3.

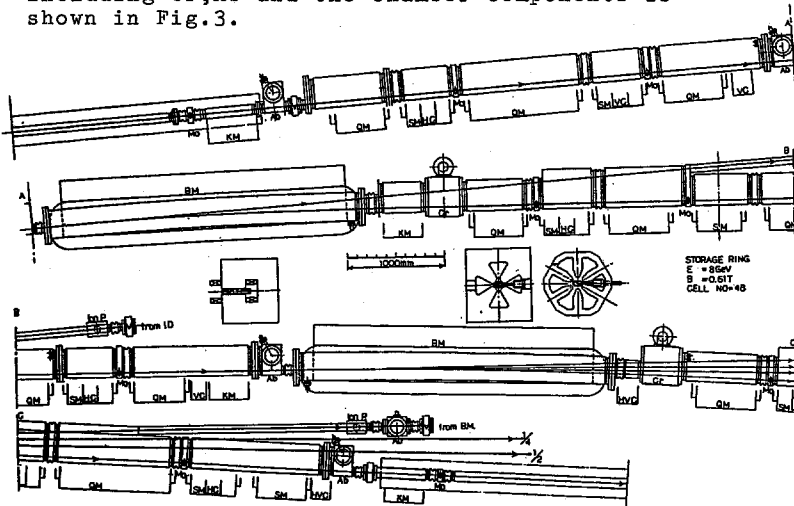


Figure 3. Schematic diagram of one cell

Our crotch, which is shown in Fig.4, consists of two water-cooled copper (OFHC) absorbers which get thermal load from the SR, and highly concentrated pumps as shown in this figure. This crotch is designed so as 1) to trap reflected photons and their associated photo-electrons, and released gas molecules, and 2) to reduce RF impedance, introduced owing to the crotch, by means of smoothing the electron beam chamber side of the trapping room including the absorber 1.

A body of the crotch is also made of copper because its photo-electron yield under SR irradiation is lower compared to that from other materials. A flange at the crotch is made of an aluminum alloy-pure aluminum-copper clad plate (by explosion method or bonding).

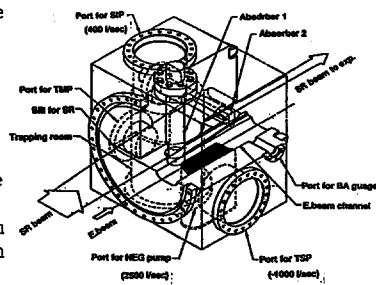


Figure 4. Isometric view of the crotch

Thermal analysis was performed in three dimensions for absorber 1 and in two dimensions for absorber 2 because of the inherent geometry of the thermal problem. Details of the calculation has been described elsewhere<sup>1</sup>. The calculation results for the absorber 1 (note that maximum SR power density is  $26 \text{ kW/cm}^2$ ) are shown in Fig.5. The maximum temperatures on the surface where the SR irradiates, are  $397^\circ\text{C}$  for the absorber 1, and  $356^\circ\text{C}$  for the absorber 2, not shown here. The maximum temperatures on the cooling wall are  $157^\circ\text{C}$  for the absorber 1 and  $117^\circ\text{C}$  for the absorber 2. This means that in case of the absorber 1, a nucleate boiling occurs at a part of the

cooling wall because the temperature of boiling point for the water pressure of  $4 \text{ kg/cm}^2$  absolute, which we set in this calculation, is  $143^\circ\text{C}$ . However,  $157^\circ\text{C}$  of the cooling wall temperature is less than  $167^\circ\text{C}$  of that corresponding to burnout.

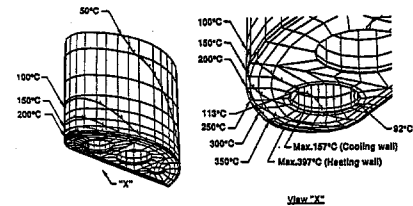


Figure 5 Calculated temperature distributions for absorber 1

### 4. CHAMBER COMPONENTS

In the design of chamber components, special effort must be given to minimize their impedance characteristics because in the storage ring, the maximum achievable beam current depends greatly on their impedance.

#### 4.1 Bellows with RF Contact

A feature of our bellows, which is shown in Fig.6, is that the RF contact is fixed at the both ends of flanges or chambers by spot welding. Thereby, we can get an electrical connection between the RF contact and flange or chamber. In the RF contacts proposed so far, their electrical connection is not clear because slider fingers at the RF contact are used.

On the other hand, our RF contact is swelled slightly in the middle at the initial state and as the bellows is contracted, the RF contact is also contracted while swelling. In the case that the bellows expands, the swelling decreases. However, this RF contact has a drawback of larger width (about 2 mm) of slits in the middle because of the larger swelling when the contact is contracted.

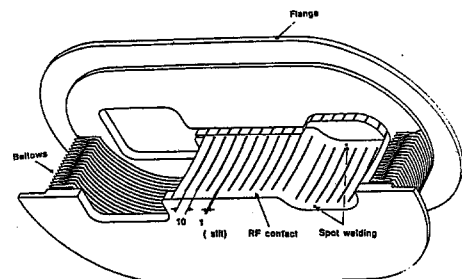


Figure 6. Bellows with RF contact

For the RF contact of 2 mm-slit width, 0.2 mm-thickness, and 5 mm-distance between the contact and bellows, we calculated H-field lines of expected four different TM modes, and show only the results for one of four TM modes in Fig.7. From Fig.7, we can find that a penetration of H-field lines into the slits, and distortion of them are not observed even at a high frequency such as 18.8 GHz. This result is in a good agreement with that obtained with the contact without the slits, not shown here. This means that even in case of 2 mm-slit width, no RF loss occurs.

The impedance contributed from the slits of the RF contact is caused by the diffraction of electromagnetic wave through them, and is of the order of  $10^{-5}$  Ohms for the bellows.

For an all metal gate valve, and a flexible vacuum chamber for ID which will be described below, we use similar RF contact to reduce the impedance.

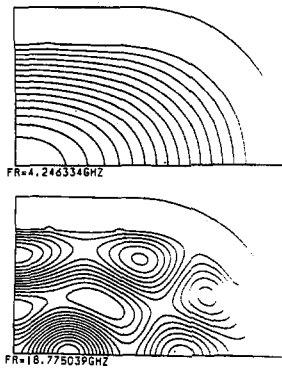


Figure 7 H-field lines in the bellows

#### 4.2 All Metal Gate Valve with RF Contact

The open position mechanism of an all metal gate valve, which is under design, is shown in Fig.8. A valve body is made of aluminum alloy except a part of valve seats and plates, and its actuation is done pneumatically. We employ a technique which provides an enclosed evacuated space between double seals, so that the leak rate from seals is decreased reducing the pressure difference across the seals.

In its open position, the RF contact which has the same geometry as the beam chamber, can bring about a direct electrical connection between two body flanges. Thus, we can avoid a step change at the valve, and eliminate the RF resistance of the body.

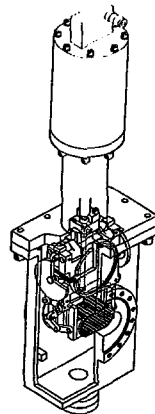


Figure 8

#### 4.3 Flexible Vacuum Chamber for ID with RF Contact

A schematic of the designed multi-period permanent-magnet ID is shown in Fig.9. The main feature is that a vacuum chamber height is variable. However, techniques 1) for manufacturing the long bellows of approximately 6 m of a race track geometry and 2) for welding between the bellows and vacuum chamber, remain to be developed.

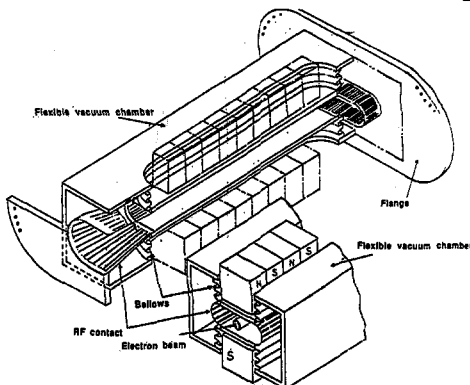


Figure 9 Flexible vacuum chamber for ID with RF contact

### 5 PUMPING SYSTEM

Our main pumping system is based on DIP installed in the bending magnet chamber and NEG strips, equipped in the straight sections which occupy most of the vacuum chamber.

The lumped NEG pump, SIP and TSP are used at the crotch and absorber locations.

As a roughing pump, turbomolecular pumps (TMP) are under consideration to be used for pumping the chambers before NEG strips, DIP, SIP and TSP start up. Furthermore, TMP's are also used for bakeout of the chambers and the activation of NEG pumps.

Pressure gradient profiles which were calculated based on the pumping system and SR power distribution, are shown in Fig.10.

In this calculation, we assumed that the distribution of SR-induced outgassing rate is in proportion to a rate of SR power deposited at crotches and absorbers, and the composition of residual gases is 80% $H_2$ +20% $CO$ . In this figure, we can find that an average pressure over the ring decreases with an increase of the integrated stored current. After 100 Ah, the average pressure is about 0.5 nTorr, and the beam lifetime of about 24 hours is expected to be achieved easily.

### 6. CONCLUSION

The current development status of vacuum system for the 8 GeV has been described. The following problems remain to be developed as tasks for R&D:

- 1) Design of a chamber for injection of electron beams,
  - 2) design of aluminum alloy flange and its sealing method,
  - 3) pretreatment of the chamber and its components,
  - 4) welding method between different metals, i.e. welding Cu-Be alloy and aluminum one,
  - 5) design of DIP, and
  - 6) design of front end of a photon beam line.
- Some part of these tasks will be designed and manufactured within the fiscal year of 1989. Prototype bending magnet- and straight section chambers have been fabricated by extrusion methods. Prototype crotch and lumped NEG pump will be completed by the end of April. Tests on these prototypes would give some results by the end of this year.

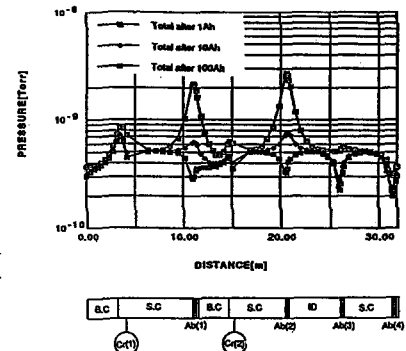


Figure 10 Pressure gradient profile per one cell

The authors are grateful to Dr H. Kamitsubo for his support for this work, Mrs T. Kusaka and T. Yoshiyuki for their calculation on RF losses and impedances.

### REFERENCES

- 1) Y. Morimoto, S. Yokouchi, H. Sakamoto, S. H. Be and T. Shirakata: To be published in RIKEN Accelerator Progress Report (1988)